1-1-2011

Dynamic Modelling of Zenith Wet Delay in GNSS Measurements

Ahmed El-Mowafy
Curtin University

Johnny Lo
Edith Cowan University

Congwei Hu
Curtin University

Dynamic Modelling of Zenith Wet Delay in GNSS Measurements

Ahmed El-Mowafy, Johnny Lo, and Congwei Hu, *Curtin University, Australia*

BIOGRAPHIES

Dr. El-Mowafy is a Senior Lecturer in the Department of Spatial Sciences, Curtin University. His area of research is positioning and navigation using GNSS, with focus on precise positioning, PPP, quality control and integration of multi-sensors for surveying and navigation applications.

Mr. Johnny Lo is a Ph.D. candidate with research interests in determination of atmospheric information using GNSS measurements.

Dr. Congwei Hu is a research fellow at the GNSS research Centre, Curtin University and holds a position as Associate Prof. at Tongji University. His area of research is precise positioning using GNSS and PPP.

ABSTRACT

Proper modelling of the temporal correlations of the zenith wet delay (ZWD) is important in some of the Global Navigation Satellite Systems (GNSS) applications such as estimation of the Perceptible Water Vapour (PWV), and methods such as Precise Point Positioning (PPP). The random walk (RW) and the first-order Gauss-Markov (GM) autocorrelation model are commonly used for the dynamic modelling of ZWD in Kalman filtering of GNSS measurements. However, it was found that the GM model consistently underestimates the temporal correlations that exist among the ZWD estimates. Therefore, a new autocorrelation dynamic model is proposed in a form similar to that of a hyperbolic function. The impact of the proposed dynamic model on the near-real time estimation of the ZWD was tested and its results were compared to that of the GM model as well as the RW model. In this test, GPS dual-frequency data collected on the 25th Jan 2010 at two Western Australian IGS stations, namely, Yarragadee and Karratha, were used. Results showed that the proposed model outperformed the GM model, and when added to hydrostatic models were able to provide near real-time (with 30 seconds intervals) ZTD estimates to within a few cm accuracy.

INTRODUCTION

In GNSS, the zenith tropospheric delay (ZTD) can be divided into two components, the hydrostatic delay and the wet delay. The zenith hydrostatic delay (ZHD) can be estimated with external models (e.g., Saastamoinen, 1973) to a few millimetres in accuracy. However, determination of the zenith wet delay (ZWD) represents a difficult task due to the dynamic nature of atmospheric water vapour. Due to changes of the temporal and spatial variability of the water vapour, the wet delay cannot be consistently modelled with millimetre precision by any existing tropospheric models. However, precise estimation of the ZWD is essential for high-precision positioning applications, the PPP technique, and Numerical Weather Prediction (NWP) modelling.

The ZWD values determined from GNSS measurements can be used to estimate the PWV. The impact of GNSS PWV estimates on weather forecasting is well documented (e.g., Kuo et al., 1996; Vedel and Huang, 2003; Gutman et al., 2004; Vedel and Huang, 2004; Vedel et al., 2004; Smith et al., 2006; Macpherson et al., 2007). These studies reported improvements in the humidity and precipitation forecasts when GNSS PWV estimates are assimilated into NWP models. The impact of GNSS PWV estimates was emphasised by a multi-year experiment over the period 1999-2004 by Smith *et al.* (2006), whereby improvements were evident in the 6-h and 12-h relative humidity forecasts. An experiment for a three month period in the corresponding campaign also witnessed the strongest improvements in the 3- and 6-hr forecasts in March-May, 2004.

A well-defined statistical description for the GNSS-derived tropospheric estimates is important for NWP modelling. The statistical correlation includes the autocorrelation, which describe the temporal correlations between pairs of GNSS tropospheric estimates in a time series as a function of time differences (Borre and Tiberius, 2000). These autocorrelation values also play a role in determining the autocorrelation time length, which can then be used in recursive data processing procedures such as GM Kalman filtering with state vector augmentation (e.g., Borre and Tiberius, 2000).

In this paper, a brief overview of the classic KF process is provided. Then, two of the more commonly-used dynamic models in the KF process, namely the RW and GM models, are outlined. A new dynamic model is then proposed to model the transition of the ZWD in the state vector of a moving entity. The proposed model is later analysed for ZWD with real GNSS data, and its results are compared to those of the RW and GM models.

KALMAN FILTERING

Kalman filtering (KF) is a technique that allows the state vector of a moving object, which is characterized by its non-stationary position and velocity, to be computed as a function of time. Kalman filter works as an adjustment process with time updates of the state vector and its covariance matrix (Hofmann-Wellenhof *et al.*, 2001), and it is often applied in real-time GNSS applications such as positioning and navigation.

The observation equation of the GNSS observations at time i (y_i) can be modelled as a function of the state vector of the unknowns (X_i) as:

$$y_i = A_i X_i + e_i \tag{1}$$

where A_i is the design matrix and e_i denotes the measurement residuals. At the initial epoch, the state vector X_0, which includes the ZWD, and its covariance matrix Q_{X_0} are assumed to be known. The state transition matrix that relates two consecutive state vectors X_i and X_{i-1} at times i and i-1 reads (Xu, 2003):

$$X_i = \Phi_{i/i-1} X_{i-1} + u_i, \quad \text{for } i = 1, 2, \ldots m \tag{2}$$

where $\Phi_{i/i-1}$ is the transition matrix. The system noise u_i is assumed to follow a normal distribution with zero mean and a known covariance matrix, Q_u. Using the covariance propagation law, the covariance matrix for the state vector in Eq. (2) is given by (Xu, 2003):

$$Q_{Xi/i-1} = \Phi_{i/i-1} Q_{X_{i-1/i-1}} \Phi^T_{i/i-1} + Q_u \tag{3}$$

Eqs. (2) and (3) are known as the time update (predicted) values for the state vector at epoch i. By applying the least-squares principle to correct for the predicted values, the estimated values of the ZWD, along with the other parameters of the state vector can be calculated by:

$$\hat{X}_{i/i-1} = \Phi_{i/i-1} \hat{X}_{i-1/i-1} \tag{4}$$

$$\hat{X}_{i/i} = \hat{X}_{i/i-1} + K\left(L_i - A_i \hat{X}_{i/i-1}\right) \tag{5}$$

$$Q_{i/i} = (I - KA_i) Q_{i/i-1} \tag{6}$$

with

$$K = Q_{i/i} A_i^T \left(A_i Q_{i/i} A_i^T + Q_{yy}\right)^{-1} \tag{7}$$

where I is the identity matrix, L_i is the misclosure vector, and Q_{yy} is the corresponding covariance matrix of measurements. The KF outlined above is of the classical case. There are several other more refined versions of the KF, such as the extended KF, the robust KF and the adaptively robust KF. Interested readers are referred to Hofmann-Wellenhof *et al.*, (2001), Xu (2003), Leick (2004) and other relevant texts for more details.

In static positioning, the positional state vector, X_i does not change with time, i.e. $X_i = X_{i-1}$, which implies that $\Phi_{i,i-1} = I$ in Eq. (2), and also, Q_u is assumed to be zero. However, the ZWD parameter will vary with time due to the fluctuations of the water vapour in the atmosphere. In this instance, an appropriate representation of the transition between adjacent ZWD measurements of sampling interval Δt is needed.

The next sections of this paper will focus only on the dynamic modelling of the ZWD through addressing the transition matrix and its corresponding stochastic parameter in the Q_u matrix. For the purpose of simplicity, the subscript i will be used instead of i/i.

Random Walk Model

A random walk (RW) model defines a random process whereby the value of the current variable, say X_i, is composed of the past variable X_{i-1} plus an error term defined as a white noise ε_i with zero mean and unit variance. Algebraically, a RW model is given by:

$$X_i = X_{i-1} + \varepsilon_i \tag{8}$$

The associated variance of the RW process noise ε_i is:

$$E\left(\varepsilon_i^2\right) = \sigma^2 \Delta t^2 \tag{9}$$

where σ^2 is the variance of the RW process noise.

First-Order Gauss Markov Model

Assuming that the correlations among the ZWD decays smoothly with time, the first-order Gauss Markov (GM) model can be called upon to describe the temporal dependence of the adjacent ZWD, such that the dynamic model of the state vector is:

$$X_i = e^{\frac{-1}{\tau_{GM}}\Delta t} X_{i-1} + u_i \tag{10}$$

where τ_{GM} is the correlation time of the GM model, and u_i is a white noise with zero mean and covariance Q_u. Figure 1 illustrates the behaviour of the GM autocorrelation function given by Eq. (10), for $\tau_{GM} = 1$ h (solid curve) and $\tau_{GM} = 2$ h (broken curve) for Δt = 30 sec.

Without loss of generality, suppose that in static processing of GNSS measurements at sites of known positions, the positional information are assumed fixed or

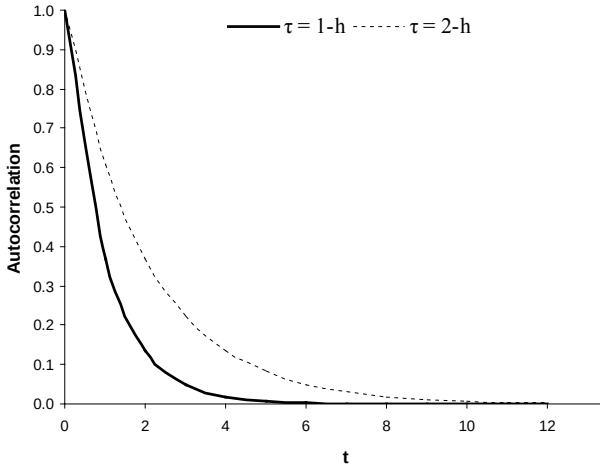

Figure 1 Autocorrelation function of GM process

tightly constrained, and that the remaining parameters, i.e. phase ambiguities, clock errors etc., are also estimated or modelled out of the observation equation beforehand. In addition, the ZHD is determined via the Saastamoinen hydrostatic model (and subtracted from the ZTD parameter prior to the estimation process). Thus, the ZWD component can be estimated from the adjustment process, e.g. KF. The GM model in Eq. (10) can be expressed for ZWD as:

$$\mathrm{ZWD_i} = e^{\frac{-1}{\tau_{GM}}\Delta t}\,\mathrm{ZWD_{i-1}} + u_i \tag{11}$$

The associated variance of the GM process noise, u_i, can be derived by firstly rearranging Eq. (11) to give:

$$u_i = \mathrm{ZWD_i} - e^{\frac{-1}{\tau_{GM}}\Delta t}\,\mathrm{ZWD_{i-1}} \tag{12}$$

Then, by squaring and taking the expectation of both sides of Eq. (12) we have:

$$\begin{aligned} E\left(u_i^2\right) &= E\left[\left(\mathrm{ZWD_i} - e^{\frac{-1}{\tau_{GM}}\Delta t}\,\mathrm{ZWD_{i-1}}\right)^2\right] \\ &= \sigma_{GM}^2\left(1 - e^{\frac{-2}{\tau_{GM}}\Delta t}\right) \end{aligned} \tag{13}$$

where σ_{GM}^2 is the steady-state variance of the GM process.

In practice, a single value for the ZWD parameter is generally estimated for a 1 h or 2 h interval (Kouba, 2009). This is due to the fact that the ZWDs generally do not vary significantly from their mean value during these short time intervals. In other words, the ZWD data behaves like a stationary process (Wei, 2006).

A PROPOSED AUTOCORRELATION MODEL

By assuming a constant mean, $\overline{\mathrm{ZWD}}$, over a short time-period, the ZWD component can be given as:

$$\mathrm{ZWD_i} = \overline{\mathrm{ZWD}} + \Delta\mathrm{ZWD_i} \tag{14}$$

Where $\Delta\mathrm{ZWD_i}$ is the difference between the ZWD value at time i and the mean value $\overline{\mathrm{ZWD}}$. The mean parameter $\overline{\mathrm{ZWD}}$ in Eq. (14) can be roughly estimated via empirical wet delay models. However, a more rigorous approach would be to estimate $\overline{\mathrm{ZWD}}$ along with $\Delta\mathrm{ZWD}$ in the Kalman filtering process. In this manner, the GM model given by Eq. (11) can then be expressed as:

$$\begin{aligned} \mathrm{ZWD_i} &= \overline{\mathrm{ZWD}} + e^{\frac{-1}{\tau_{GM}}\Delta t}\,\Delta\mathrm{ZWD_{i-1}} + \tilde{u}_i \\ &= \overline{\mathrm{ZWD}} + \Phi_{i,i-1}\Delta\mathrm{ZWD_{i-1}} + \tilde{u}_i \end{aligned} \tag{15}$$

where $\tilde{u}_i$ is a white noise with zero mean and variance $\sigma_{\tilde{u}}^2$. The associated variance $\sigma_{\tilde{u}}^2$ for $\Delta\mathrm{ZWD}$ is identical to that given by Eq. (13).

The GM autocorrelation function given by Eq. (10) is dependent on the empirical value given to the correlation time τ_{GM}. The value for τ_{GM} can be directly estimated from the GM autocorrelation function:

$$\rho(\Delta t) = e^{\frac{-1}{\tau_{GM}}\Delta t} \tag{16}$$

given at the $\rho = 1/e$ point when $\tau_{GM} = \Delta t$. Alternatively, it can be determined at a specific time lag where significant ZWD autocorrelation is no longer observed. For instance, Figure 2 shows the autocorrelation of PWV with lags of 1 h intervals, which can be transformed to ZWD (and vice versa), at ALIC station in Australia at three different dates (31 March, 3rd April, and 6th April 2010). From the figure, τ can be determined by finding the intersection between the autocorrelation trend line and the confidence interval (broken red line), which vary, within a small range, between different tests. From the figures, the value of τ can be taken between 1 and 2 hours.

An alternative autocorrelation function is proposed in this study that can be used in the transition matrix. By studying the autocorrelation of ZWD of several data sets, it was found that the trend exhibited by a hyperbolic function gives a reasonable representation of this autocorrelation changes. Thus, the proposed autocorrelation function between the ZWDs at epochs i and i-k, i.e. for a lag $\Delta t = k$, can be given by:

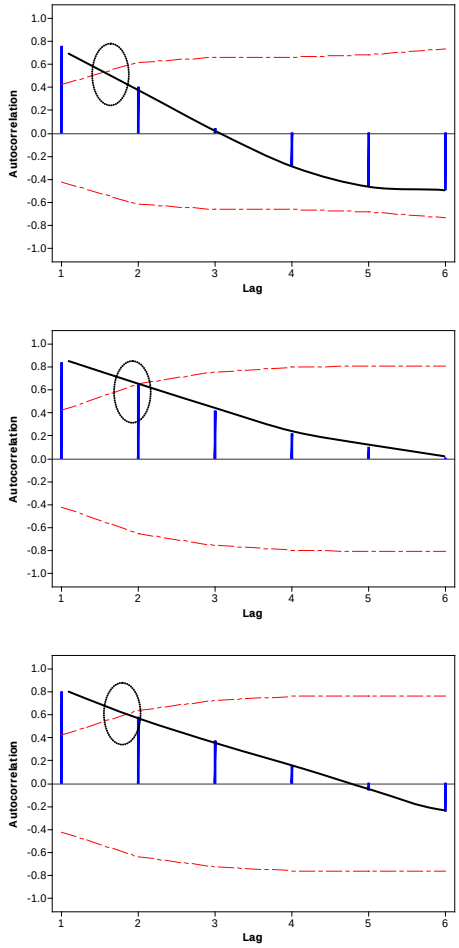

Figure 2 Autocorrelation plot of the PWV estimates over ALIC on 31st Mar, 3rd Apr, and 6th Apr.

$$\text{Correlation}\left(ZWD_i, ZWD_{i-k}\right) = \rho(\Delta t) = \frac{1}{\left(\frac{\Delta t}{\tau_{PM}} + 1\right)^{\left(\frac{\Delta t}{\tau_{PM}}\beta\right)}} \quad (17)$$

where τ_{PM} is the correlation time of the proposed model, and the parameter β is chosen from experience based on the analysis of several data sets or to be determined from the data at hand as given below. To estimate β, a set of *n* autocorrelation estimates for an initial period of ZWD data set can be determined using a standard autocorrelation approach. That is,

$$\rho(\Delta t) = \frac{\hat{Z}(\Delta t)}{\hat{Z}(0)} \quad (18)$$

with

$$\hat{Z}(\Delta t) = \frac{1}{n}\sum_{i=1}^{n-\Delta t}\left(ZWD(t) - \overline{ZWD}\right)\left(ZWD(t+\Delta t) - \overline{ZWD}\right) \quad (19)$$

where $\overline{ZWD}$ is the empirical mean. Taking the natural logarithm of both sides of Eq. (17) results in the linearised form:

$$\ln(\rho) = \left[-\left(\frac{\Delta t}{\tau_{PM}}\right) \times \ln\left(\frac{\Delta t}{\tau_{PM}} + 1\right)\right]\beta \quad (20)$$

An estimate for β, i.e. $\hat{\beta}$, can then be calculated by performing least-squares analysis on the first $n/12$ number of autocorrelation values, generated by Eqs. (17) and (18), using the linear relationship defined by Eq. (20). In real-time applications, a default value of β can be used during this period until $\hat{\beta}$ is computed. Once $\hat{\beta}$ has been determined, the proposed model (PM) given by Eq. (17) is then fully defined.

As stated earlier, an important application of determining ZWD from GNSS measurements is to estimate PWV. Figures 3 to 6 demonstrate the capability of the proposed model in following the trend of autocorrelations, which were calculated via Eq. (18) from the actual PWV values determined from radiosonde data. The plots are given at four different locations (Alice Springs, Broome, Burnie and Ceduna) across Australia. The GM model is also included in these figures for comparison purposes. For the GM model, the value of τ_{GM} is determined at a time lag t where (statistically) significant autocorrelation is observed using the Ljung-Box Q statistic (Ljung and Box, 1978). For the proposed model, τ_{PM} is taken equals τ_{GM}.

From Figures 3 to 6, it can be seen that the GM function did not adequately represent the actual PWV autocorrelations. The GM function consistently over-estimates the rate at which the PWV autocorrelation values decreases. Conversely, the proposed model, given by Eq. (17) is able to provide autocorrelation values that closely follow the actual autocorrelation values for a significant length of time.

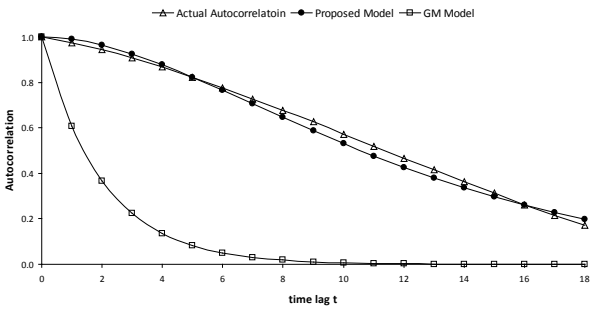

Figure 3 Comparison between the proposed model (solid circles) and the GM model (squares) in estimating the actual PWV autocorrelations (triangles) at Alice Springs (NT)

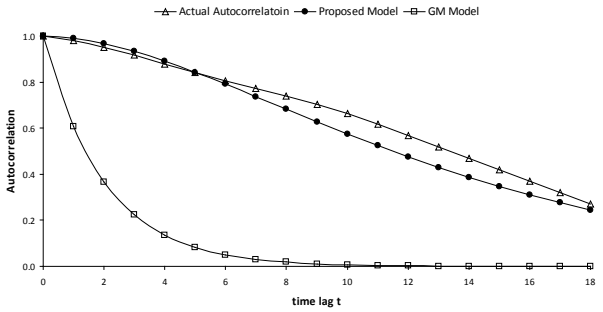

Figure 4 Comparison between the proposed model and the GM model in estimating the actual PWV autocorrelations at Broome (Western Australia)

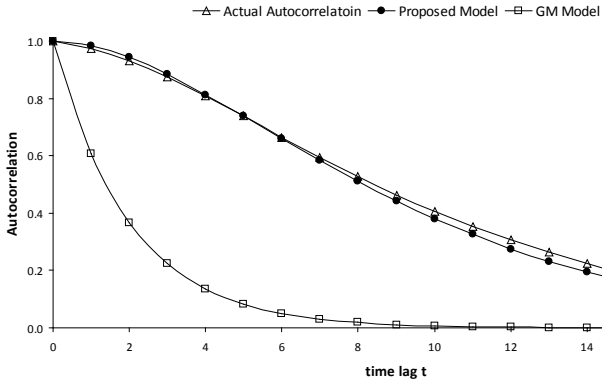

Figure 5 Comparison between the proposed model and the GM model in estimating the actual PWV autocorrelations at Burnie (Tasmania).

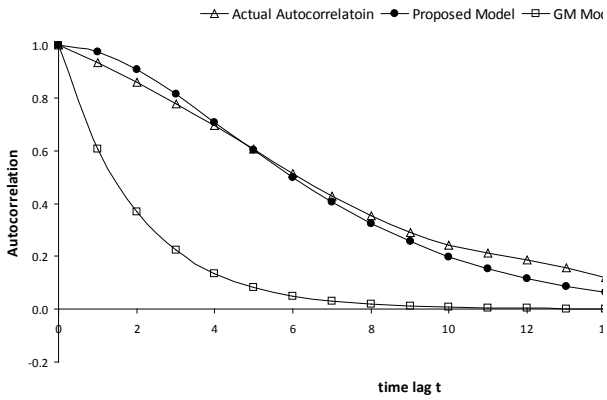

Figure 6 Comparison between the proposed model and the GM model in estimating the actual PWV autocorrelations at Ceduna (South Australia)

For the proposed autocorrelation model, the state element of the ZWD at time i can be represented by:

$$\mathrm{ZWD}_i = \frac{1}{\left(\frac{\Delta t}{\tau_{PM}}+1\right)^{\left(\frac{\Delta t}{\tau_{PM}}\beta\right)}} \times \mathrm{ZWD}_{i-1} + u_i \qquad (21)$$

To determine the variance of the process noise Q_u, the quantity u_i in Eq. (21) is once again isolated, then taking the expectation of its square gives:

$$E\left(u_i^2\right) = E\left[\left(\mathrm{ZWD}_i - \frac{1}{\left(\frac{\Delta t}{\tau_{PM}}+1\right)^{\left(\frac{\Delta t}{\tau_{PM}}\beta\right)}} \times \mathrm{ZWD}_{i-1}\right)^2\right]$$

$$= \sigma^2\left[1 - \left(\frac{1}{\left(\frac{\Delta t}{\tau_{PM}}+1\right)^{\left(\frac{2\Delta t}{\tau_{PM}}\beta\right)}}\right)\right] \qquad (22)$$

where σ^2 is the variance of the process. The ZWD state element, given in Eq. (21), can also be represented in the form described in Eq. (15).

NEAR REAL-TIME ESTIMATION OF THE ZENITH WET DELAY AT A SINGLE STATION

The Gauss-Markov model given in Eq. (10) uses the temporal correlations that exist among the ZWD estimates to provide near real-time (NRT) wet delay estimates in the Kalman filter process. However, it was shown in the previous section that, for the presented data, the corresponding GM autocorrelation function did not adequately represent the autocorrelation trend as it consistently underestimated the actual ZWD autocorrelation values. An alternative autocorrelation function was therefore proposed. The proposed autocorrelation function was shown to follow the ZWD autocorrelation trend more closely than that of the GM function in the post-mission mode. However, its effect on the NRT estimation of the ZWD is still not presented. Hence, in this section, the impact of the proposed model (PM) on the NRT estimation of the ZWD is tested. The corresponding results are next compared to that of the GM model as well as the random-walk (RW) model given by Eq. (8) as these models are the current widely used models for ZWD estimation.

In this investigation, 24 h of GNSS dual-frequency data with 30 seconds sample intervals on the 25th Jan 2010 from two Western Australian IGS stations, namely Yarragadee (YAR2) and Karratha (KARR), were used to test the models. The stations were processed independently in the PPP mode. IGS products, including the IGS final orbital file, satellite clock information, Earth Orientation Parameters (EOPs), the coordinates of the

ground stations and the antenna phase centre offsets and variations were used (El-Mowafy, 2009). An elevation angle cut-off of 5^o and the Niell mapping functions (Niell, 1996) were used in processing of the GNSS data. The ionosphere-free linear combination of GNSS observations was implemented to mitigate the first-order ionospheric residual errors. In conjunction with the standard surface meteorological data, i.e. 20^o C in temperature, 50% humidity and 1010 millibars in pressure, the Saastamoinen hydrostatic model (Saastamoinen, 1973) was used to provide *a-priori* ZHD estimates, which usually have accuracy of better than 95%. These ZHD estimates, with the aid of the mapping functions, were then subtracted from the observations, leaving mainly behind the ZWD parameters, which are to be estimated. The KF process, was used to estimate the ZWD at every 30-second interval, along with the station coordinate partials, ambiguities and receiver clock error in a PPP mode. The RW, GM and proposed models were used for dynamic modelling of ZWD in three separate runs of KF. The station coordinates were not assumed fixed, as this investigation is carried out to simulate kinematic positioning. For the GM model and the PM, two KF approaches were used:

(1) Estimate the ZWD term as a random process in the form:

$$ZWD_i = \frac{1}{\left(\frac{\Delta t}{\tau_{PM}}+1\right)^{\left(\frac{\Delta t}{\tau_{PM}}\beta\right)}} ZWD_{i-1} + u_i \qquad (23)$$

(2) Estimate the ZWD parameter in terms of the mean ZWD and the residual simultaneously, i.e. in the form:

$$ZWD_i = \overline{ZWD} + \frac{1}{\left(\frac{\Delta t}{\tau_{PM}}+1\right)^{\left(\frac{\Delta t}{\tau_{PM}}\beta\right)}} \Delta ZWD_{i-1} + \tilde{u}_i \qquad (24)$$

Prior to this investigation, an autocorrelation analysis of the PWV estimates across 10 Australian stations was carried out. Based on the analysis of the ZWD autocorrelation results, the correlation time τ for both the GM model and the proposed model was empirically taken as 4800 seconds. The empirical β value for the PM is taken as $3/4$. Once the ZWD is estimated, it is then added to the estimated ZHD, and hence, the ZTD can be computed. The estimated ZTD from each of the models are averaged at every 5 min and at every 2-h periods, respectively, during the course of the 24-h test period and are then compared to the IGS tropospheric solutions. Tables 1 and 2 present the Root Mean Square Error (RMSE) of the differences between the estimated ZTD and the 5-min IGS ZTD solution, whilst Table 2 provides the RMSE of the estimated ZTD when compared with the 2-h IGS solution. The table gives results when assuming 2 mm, 5 mm, and 10 mm standard deviation of the process noise for ZWD. GM1 and PM1 are; respectively, the GM model and PM processed with the *first* approach given in Eq. (11) and (23). Similarly, GM2 and PM2 are; respectively, the GM model and PM processed with the *second* approach given in Eq. (15) and (24).

Tables 1 and 2 indicate that there are marginal RMSE differences when the estimated ZTD were compared to the 5-min and the 2-h IGS solutions across both stations. The maximum difference between the RMSE values is 2.4 mm, with an average difference of 0.7 mm. Figure 7 provides a plot of the spread of the RMSE difference.

Table 1 RMSE (mm) of the differences between the estimated ZTD and the IGS solutions (5-min)

			1 mm SD		
Station	**RW**	**GM1**	**GM2**	**PM1**	**PM2**
YAR2	17.2	72.4	16.1	16.2	14.3
KARR	17.1	126.8	28.6	21.8	20.5
			5 mm SD		
Station	**RW**	**GM1**	**GM2**	**PM1**	**PM2**
YAR2	15.3	55.2	13.6	14.7	14.4
KARR	11.4	99.2	11.1	10.1	14.7
			10 mm SD		
Station	**RW**	**GM1**	**GM2**	**PM1**	**PM2**
YAR2	15.6	43.1	14.4	15.1	15.8
KARR	14.9	79.4	13.9	13.5	18.8

Table 2 RMSE (mm) of the differences between the estimated ZTD and the IGS solutions (2-h))

			1 mm SD		
Station	**RW**	**GM1**	**GM2**	**PM1**	**PM2**
YAR2	15.8	71.4	15.2	14.6	12.2
KARR	15.7	126.4	26.5	20.7	18.9
			5 mm SD		
Station	**RW**	**GM1**	**GM2**	**PM1**	**PM2**
YAR2	14.0	53.9	13.3	13.4	13.6
KARR	12.2	97.6	10.9	10.3	15.5
			10 mm SD		
Station	**RW**	**GM1**	**GM2**	**PM1**	**PM2**
YAR2	15.2	40.9	14.3	14.7	15.6
KARR	15.9	76.9	14.9	14.2	19.3

When estimating the ZWD parameter as a random process in the first approach, the GM model (GM1) was the worst performer. The corresponding RMSE for GM model

ranged from about 4 cm to 12 cm. The PM1, generally produced the best results at both stations, with the corresponding ZTD RMSE values ranging from about 1 cm to 2 cm. Overall, the results of the RW were marginally bettered by the PM. The best results for the RW model and the PM1 were achieved at standard deviation of 5 mm.

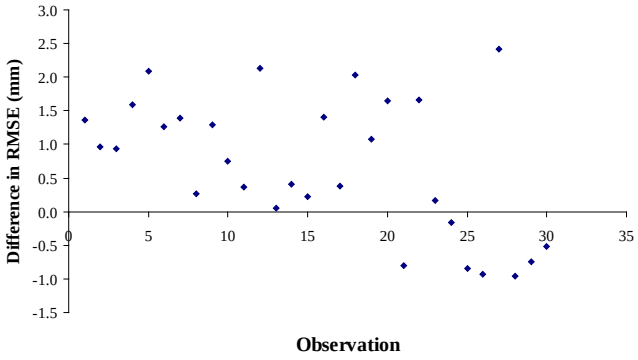

Figure 7 Differences between the (estimated ZTD – 5-min IGS ZTD) RMSE and the (estimated ZTD – 2-h IGS ZTD) RMSE

In the second KF approach whereby the mean ZWD, i.e. $\overline{\text{ZWD}}$, is estimated along with the residual ZWD, i.e. ΔZWD, the performance of the GM model has dramatically improved from 4 cm to 12 cm in the initial approach to around 1.3 cm to 2.9 cm across both stations. The final results of the GM2 model are comparable to that of the PM1 and the RW model. A difference of up to 5 mm can be observed between the PM1 and the PM2 model, with the latter being less accurate. However, this can be explained by examing the parameterisation of the $\overline{\text{ZWD}}$ and ΔZWD in the corresponding design matrix, given by Eq. (15). In modelling the $\overline{\text{ZWD}}$, the coefficients of the corresponding column in the design matrix are defined as a vector of ones. The coefficients for the ΔZWDs, which are modelled by the PM, are close to one due to the high correlation that exists between successive ZWD estimates since the sampling interval was only 30 s. The design matrix will therefore includes two columns that are almost similar. Thus, to avoid singularity in this case, the use of the PM with the ZWD that is decomposed into two componets, $\overline{\text{ZWD}}$ and ΔZWD, is recommended only for longer time intervals. Figure 8 shows that overall across both stations, the RW and PM1 models have yielded the best results.

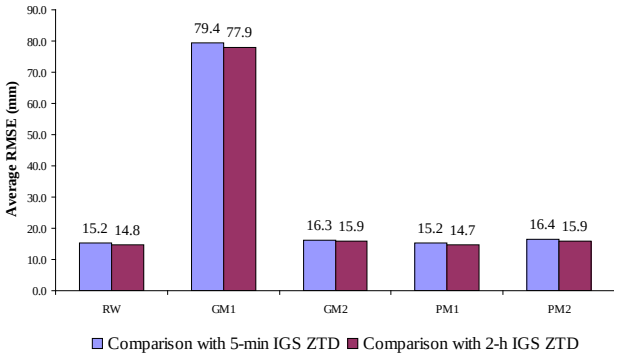

Figure 8 Average (estimated ZTD – 5-min IGS ZTD) RMSE (mm) and (estimated ZTD – 2-h IGS ZTD) RMSE at YAR2 and KARR

SUMMARY

In the kinematic modelling of the GNSS measurements, the remaining part of ZTD after modelling out the ZHD involves mainly the ZWD, which does not vary significantly from its mean value during short time intervals. Thus, the ZWD can be considered as comprising two components, a mean value that is taken constant over short time-periods, and a variable component that is modelled as a random process with zero mean. Both components need to be determined in the processing algorithm (e.g. Kalman filtering), and thus, their dynamic and stochastic models should be identified. The dynamic function of the constant part is simply taken one, with zero variance. The first-order Gauss-Markov (GM) autoregressive function can be used for modelling the dynamic behaviour of the random process component. To investigate this assumption, the actual PWV from radiosonde data were collected at four different locations across Australia (Alice Springs, Broome, Burnie and Ceduna) and the trend of their computed autocorrelations were compared with autocorrelations determined from the GM model. It was found that the GM model consistently underestimates the temporal correlations of the PWV measurements. Therefore, a new autocorrelation dynamic model is proposed. The proposed autocorrelation function gave results in good agreement with the autocorrelation changes of the actual PWV for the test data considered.

The impact of the proposed dynamic model on the near-real time estimation of the ZWD was also tested and its results were compared to that of the GM model as well as the random walk model. In this test, 24 hours of GPS dual-frequency data collected on the 25th Jan 2010 at two Western Australian IGS stations, namely Yarragadee and Karratha were used. The stations data were processed independently in a PPP mode using each of the three models. The published IGS final ZTD at the two stations were used as a reference for comparison of the results from the three models.

In estimation of the ZWD, two approaches were considered. The first is a classical approach where ZWD is modelled as one variable. In the second, the proposed estimation approach was implemented, where the mean ZWD is estimated along with the residual random process component. Results at the two stations showed that for the first approach, the corresponding RMSE for GM model ranged from about 4 cm to 12 cm. The proposed autocorrelation model generally produced the best results at both stations, with the corresponding ZTD RMSE values ranging from about 1 cm to 2 cm. In the second approach, where the ZWD is estimated as a mean value and a random process, the performance of the GM model has significantly improved to around 1.3 cm to 2.9 cm for both stations whereas the performance of the proposed autocorrelation model had no improvement. Future work includes testing the proposed model on longer datasets, at different locations with globe distribution, and under various operational and site conditions.

ACKNOWLEDGMENTS

This work is supported by an Australian Research Council APAI grant No. LP0347723, in collaboration with the Australian Bureau of Meteorology, and a PhD scholarship from the Department of Spatial Sciences, Curtin University, Perth, Australia. The financial support from The Institute of Geoscience Research (TIGeR), Curtin University, to present the paper is acknowledged.

REFEREMCES

Borre, K., and C. Tiberius. 2000. *Proceedings of the 11th International Technical Meeting of the Satellite Division of The Institute of Navigation*, *Time series analysis of GPS* observables. Salt Lake City, Utah: ION GPS-2000

El-Mowafy, A. 2009. An Alternative Post-Processing Relative Positioning Approach Based on Precise Point Positioning. *Journal of Surveying Engineering, ASCE*, 135 (2): 56-65.

Gutman, S. I., S. R. Sahm, S. G. Benjamin, B. E. Schwartz, K. L. Holub, J. Q. Stewart, and T. L. Smith. 2004. Rapid retrieval and assimilation of ground based GPS precipitable water observations at the NOAA forecast systems laboratory: Impact on weather forecasts. *Journal of the Meteorological Society of Japan* 82 (1B): 351-360.

Hofmann-Wellenhof, B., H. Lichtenegger, and J. Collins. 2001. *GPS theory and practice*. 5th ed. New York: Springer-Verlag Wien.

Kouba, J. 2009. A guide to using International GNSS Service (IGS) Products. (last accessed 21/9/09) http://acc.igs.org/UsingIGSProductsVer21.pdf.

Kuo, Y. H., X. Zou, and Y. R. Guo. 1996. Variational assimilation of precipitable water using a nonhydrostatic mesoscale adjoint model. *Monthly Weather Review* 124 (1): 122-147.

Leick, A. 2004. *GPS Satellite Surveying*. 3rd ed. New Jersey, USA: John Wiley & Sons, Inc.

Ljung, G. M., and G. E. P. Box. 1978. On a measure of a lack of fit in time series models. *Biometrika* 65: 297-303.

Macpherson, S. R., G. Deblonde, J. M. Aparicio, and B. Casati. 2007. Impact of NOAA ground-based GPS observations on the Canadian regional analysis and forecast system. *Monthly Weather Review* 136 (7): 2727-2745.

Niell, A. E. 1996. Global mapping functions for the atmosphere delay at radio wavelenghts. *Journal of Geophysical Research* 101 (B2): 3227-3246.

Saastamoinen, J. 1973. Contributions to the theory of atmospheric refraction. *Bullétin Géodésique* 105, 106, 107: 279-298, 383-397, 13-34.

Smith, T. L., S. G. Benjamin, S. I. Gutman, and S. Sahm. 2006. Short-range forecast impact from assimilation of GPS-IPW observations into the Rapid Update Cycle. *Monthly Weather Review* 135 (8): 2914–2930.

Vedel, H., and X. Y. Huang. 2003. A NWP impact study with ground based GPS data. In *The International Workshop on GPS Meteorology*. Tsubaka, Japan.

Vedel, H., and X. Y. Huang. 2004. Impact of ground-based GPS data on numerical weather prediction. *Journal of Meteorological Society of Japan* 82 (1B): 459-472.

Vedel, H., X. Y. Huang, J. Haase, M. Ge, and E. Calais. 2004. Impact of GPS zenith tropospheric delay data on precipitation forecasts in Mediterranean France and Spain. *Geophysical Research Letters* 31: L02102.

Wei, W. 2006. *Time series analysis - Univariate and multivariate methods*. 2nd ed. USA: Pearson Education, Inc.

Xu, G. 2003. *Theory, Algorithms and Applications*. Berlin: Springer.